Effects of nuclear deformation on the form factor for direct dark matter detection*

CHEN Ya-Zheng(陈亚正)[1)] CHEN Jun-Mou(谌俊谋) LUO Yan-An(罗延安)
SHEN Hong(申虹) LI Xue-Qian(李学潜)

School of Physics, Nankai University, Tianjin 300071, China

Abstract: For the detection of direct dark matter, in order to extract useful information about the fundamental interactions from the data, it is crucial to properly determine the nuclear form factor. The form factor for the spin-independent cross section of collisions between dark matter particles and the nucleus has been thoroughly studied by many authors. When the analysis was carried out, the nuclei were always supposed to be spherically symmetric. In this work, we investigate the effects of the deformation of nuclei from a spherical shape to an elliptical one on the form factor. Our results indicate that as long as the ellipticity is not too large, such deformation will not cause any substantial effects. In particular, when the nuclei are randomly orientated in room-temperature circumstances, one can completely neglect them.

Key words: nuclear density, dark matter

PACS: 21.10.Ft, 95.35.+d **DOI:** 10.1088/1674-1137/36/6/005

1 Introduction

Due to serious astronomical observations over several decades, the existence of dark matter is no longer in doubt. On the other hand, we definitely know that in the zoo of the standard model (SM), we do not have any candidates for dark matter (DM). The question then arises as to what the dark matter particles are? There have been many models proposed in the literature [1–7], but unless they are captured by our detectors in terrestrial laboratories or satellites [8–10], surely one still cannot identify them. More efforts have been made to discover dark matter flux from outer space.

Compared with the spin-dependent cross section, the spin-independent cross section of dark matter particles with a nucleus is much larger due to A^2 enhancement, where A is the atomic mass number of the nucleus as the detection material [11–17]. Even so, the cross sections of elastic scattering between DM particles and nuclei are still small, and the present experiments have already reached 10^{-44} cm^2. Because of the advantages of spin-independent scattering, whose cross sections are larger, and because theoretical treatments are more simple than those for spin-dependent processes, nowadays research priority is given to the study of spin-independent elastic DM-nucleus reactions.

Since the kinetic energy of the DM particle is rather low at the order of a few tens of keV, it is almost impossible for the impact of the DM particle on the nucleus to cause inelastic processes, and thus all observational signals are related to the recoil of the nucleus after the collision. The elementary processes are the collisions between DM and quarks (not gluons at the tree level). Because the available kinetic energy is rather low, all the energy absorbed by the quarks would be totally passed to the nucleon in which the quarks reside, and then to the nucleus without exciting the nucleon and nucleus. Namely the processes are elastic at all the three different stages: collision between DM and quark; DM and nucleon; DM and nucleus. The observable effects are the elastic scattering of the DM particle with the nucleus. The nucleus is recoiling as a whole object to induce thermal, electronic and light signals which can be caught by earth detectors. For the spin-independent cross section, the particle-physics and nuclear-physics contributions

Received 12 December 2011

* Supported by National Natural Science Foundation of China (11075079, 11075080, 11075082)

1) E-mail: cyzufo@mail.nankai.edu.cn

can be separated, namely the nuclear effects can be factored out and included in a form factor $F(\boldsymbol{q})$. For spherically symmetric nuclei, $F(\boldsymbol{q})$ only depends on $|\boldsymbol{q}|$. The spherical symmetry means that the nuclei are full-shell or close to full-shell structures, but for most of the nuclei that are taken as the detection materials, the shells are not completely filled out. A careful study of the form factors for the non-full-shell structure nuclei would be helpful in extracting information about the fundamental interactions from the data. In that case, $F(\boldsymbol{q})$ is not only a function of $|\boldsymbol{q}|$, but also $\cos\theta$, while the azimuthal symmetry is assumed. We will write this as $F(q,\ \cos\theta)$, where $q\equiv|\boldsymbol{q}|$.

A nucleus is a complex many-body system, and therefore extraction from the data requires a thorough analysis of nuclear structure. The form factors for spherical nuclei have been carefully studied by many authors, and the results can be applied to analysis of the data. In this work, we are going to investigate the effects of the deformation of nuclei on the form factor, namely, we will derive the form factors corresponding to the deformed nuclei with relatively small ellipticity.

We employ several models to calculate the form factors $F(q,\ \cos\theta)$ for nuclei with small ellipticity. We will take Xe and Ge, which are commonly adopted as detection materials, as examples to illustrate the effects of deformation.

The paper is organized as follows. After this introduction, we present the expressions of the form factors derived from different models for nuclear density, and then present our numerical results via several figures. The last section is devoted to our conclusion and discussion.

2 The form factor related to a deformed nucleus

Obviously, it is reasonable to assume that a nucleus with a larger A may only be quadruply deformed, namely, it is deformed from a spherical to an ellipsoidal form. In the spherical coordinates, the nuclear density of a nucleus with an elliptical form should be $\rho(r,\theta)$, which is a function of both radius r and polar angle θ, and the corresponding form factor should be written as follows. It should be noted that we would set $\varphi_1=\varphi_2$ in practical calculations to simplify the integration.

$$\begin{aligned}F(q,\theta_2) &= \frac{1}{M}\int\rho(r,\theta_1)\mathrm{e}^{\mathrm{i}\vec{q}\cdot\vec{r}}\mathrm{d}^3r \\ &= \frac{1}{M}\int_0^{\pi}\sin\theta_1\mathrm{d}\theta_1\int_0^{2\pi}\mathrm{d}\varphi_1\int_0^{\infty}\rho(r,\theta_1)\mathrm{e}^{\mathrm{i}qr(\sin\theta_1\sin\theta_2\cos(\varphi_1-\varphi_2)+\cos\theta_1\cos\theta_2)}r^2\mathrm{d}r. \end{aligned} \quad (1)$$

Even though this work aims to find the effects of the deformation of nuclei on the form factor, the deviation from the spherical form for the nuclei under investigation is not severe, therefore, we can always start from a spherical form and then make reasonable modifications or extensions.

2.1 Extension of the two-parameter Fermi distribution (E2PF)

A number of models have been proposed [18, 19] to describe the nuclear charge density or mass density. Among them, the two-parameter Fermi distribution (2PF) is one of the simplest models. For a spherical form, the density is written as

$$\rho(r)=\frac{\rho_0}{1+\exp\left(\dfrac{r-c}{z}\right)}, \quad (2)$$

where ρ_0 is equal to $2\rho(r)$ at $r=c$, and z is the diffusivity of the surface. It would be convenient for later use to derive the mean square root radius $\bar{R}$ for the spherical 2PF model as

$$\bar{R}^{\mathrm{2PF}}=\sqrt{\frac{4\pi\displaystyle\int_0^{\infty}r^4\rho(r)\mathrm{d}r}{4\pi\displaystyle\int_0^{\infty}r^2\rho(r)\mathrm{d}r}}=\sqrt{\frac{3}{5}c^2+\frac{7}{5}\pi^2z^2}. \quad (3)$$

For an elliptical nucleus with an axial symmetry, the nuclear density in the two-parameter Fermi distribution (E2PF) model should be extended as [20–27]:

$$\rho(r,\theta)=\frac{\rho_0'}{1+\exp\left(\dfrac{r-c(\theta)}{z}\right)}, \quad (4)$$

where

$$c(\theta)=c_0(1+\beta_2Y_{20}(\theta)). \quad (5)$$

The parameter β_2, which corresponds to the ellipticity of the nucleus characterizing its deformation from a spherical form, is a small quantity for the nucleus with which we are concerned. For the priori assumption of small deformation, we only keep the multiple terms up to Y_{20} [27].

The parameters $c_0 = 1.1A^{1/3}$ and ρ'_0 can be obtained by the normalization condition, i.e. requiring integration over the whole coordinate space to be equal to the nuclear mass number (or total charge Ze), which is priori set for various nuclei. β_2 can be obtained from the data book [28], and is -0.113 and -0.224 for ^{131}Xe and ^{73}Ge, respectively. z denotes the surface diffuseness. Here we choose the normalization as follows:

$$\int \rho(r,\theta)\mathrm{d}^3r = M. \tag{6}$$

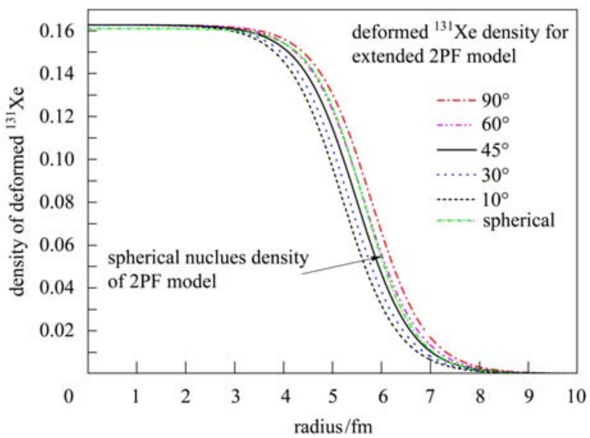

Fig. 1. The nuclear density of ^{131}Xe for the extended 2PF model, showing the change in density with increasing angle from 10° to 90°. The short dashed-dotted line (green) corresponds to the case of the spherical 2PF model.

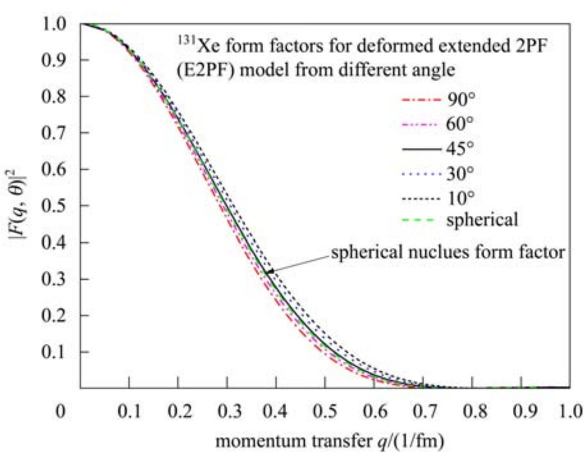

Fig. 2. ^{131}Xe form factors for the deformed nucleus extended 2PF(E2PF) model from different directions: 10°, 30°, 45°, 60°, 90°.

In Fig. 1 we show the density distribution for ^{131}Xe in the E2PF model. It is observed that from the center of the nucleus to about three fermis, the density remains unchanged in all directions. Then the angular distribution of the density begins to move apart for different angles beyond three fermis. The short dashed-dotted (green) line shows the 2PF density model when the nucleus is assumed to be spherical. Fig. 2 is the corresponding form factors, which are calculated by taking a Fourier transformation to the deformed nuclear density in the configuration space.

2.2 Extension of the folding model (EF)

There is another commonly adopted model which is rather simple, i.e. the nucleons are postulated to be uniformly distributed in a sphere with a certain boundary radius. For an axially symmetric ellipsoidal shape, one should extend the density for a spherical form. The surface equation of an ellipsoid is

$$\frac{x^2}{a^2}+\frac{y^2}{a^2}+\frac{z^2}{b^2}=1, \tag{7}$$

or in the spherical coordinate system, it is written as

$$R(\theta)=\sqrt{\frac{a^2b^2}{(a^2-b^2)\cos^2\theta+b^2}}. \tag{8}$$

In an approximation, if we only keep the multiple terms to quadrupole, we can re-parametrize the surface equation to a more convenient one,

$$R(\theta)=R_0(1+\beta_2 Y_{20}). \tag{9}$$

Extending the folding model, we set the nuclear density to be uniform inside the ellipsoid with radius $R(\theta)$

$$\rho_0(r,\theta)=\frac{3M}{4\pi a^2 b}\Theta(r-R(\theta)), \tag{10}$$

where Θ is the step function. Following the literature [29], we introduce a smearing function ρ_1 to take care of the soft edge effect of the nucleus:

$$\rho_1(r)=\frac{1}{(2\pi s^2)^{3/2}}\exp\left(\frac{-r^2}{2s^2}\right), \tag{11}$$

then one should convolve ρ_0 and ρ_1 to get the nuclear density

$$\begin{aligned}\rho(r,\theta) &= \int\rho_0(\vec{r'})\rho_1(\vec{r}-\vec{r'})\mathrm{d}^3r' = \int\rho_0(\vec{r'})\rho_1(\vec{r}-\vec{r'})r'^2\mathrm{d}r'\sin\theta'\mathrm{d}\theta'\mathrm{d}\varphi' \\ &= \frac{1}{(2\pi s^2)^{3/2}}\int_0^{2\pi}\mathrm{d}\varphi'\int_0^{\pi}\sin\theta'\mathrm{d}\theta'\int_0^{\infty}\frac{3M}{4\pi a^2 b}\Theta(r'-R(\theta')) \\ &\quad\times\exp\left(\frac{-(r^2+r'^2-2rr'(\sin\theta\sin\theta'\cos(\varphi-\varphi')+\cos\theta'\cos\theta))}{2s^2}\right)r'^2\mathrm{d}r'.\end{aligned} \tag{12}$$

The semi-axes a and b are set as

$$\begin{aligned} a &= R\left(\theta=\frac{\pi}{2}\right)=R_0\left(1+\beta_2 Y_{20}\left(\frac{\pi}{2}\right)\right) \\ &= R_0\left(1-\sqrt{\frac{5}{16\pi}}\beta_2\right) \\ b &= R(\theta=0)=R_0(1+\beta_2 Y_{20}(0)) \\ &= R_0\left(1+2\sqrt{\frac{5}{16\pi}}\beta_2\right). \end{aligned} \tag{13}$$

In the extended folding (EF) model, we can also calculate the mean square root radius $\bar{R}^{\mathrm{EF}}$. For a spherical nucleus, one may equate the mean square root radius obtained in the 2PF and folding models, thus acquiring the spherical radius R_0 for the folding model [18, 30].

$$R_0=\sqrt{c^2+\frac{7}{3}\pi^2a^2-5s^2}, \tag{14}$$

$c\simeq(1.23A^{1/3}-0.6)$ fm, $s=0.9$ fm, $a=0.52$ fm.

As mentioned previously, the deformation makes the shape of the nucleus deviate slightly from a spherical form. We can still use the above relation achieved for spherical nuclei and set R_0 to be the parameter in Eq. (9).

A Fourier transformation would bring the nuclear density to the expected form factor $F(q,\theta)$. It is noted that now the form factor is also direction-dependent.

$$\begin{aligned} F(q) &= \int\rho_0(\boldsymbol{r}')\rho_1(\boldsymbol{r}-\boldsymbol{r}')\mathrm{d}^3r'\mathrm{e}^{\mathrm{i}\boldsymbol{q}\cdot\boldsymbol{r}}\mathrm{d}^3r \\ &= \int\rho_0(\boldsymbol{r}')\mathrm{d}^3r'\int\rho_1(\boldsymbol{r}-\boldsymbol{r}')\mathrm{d}^3r'\mathrm{e}^{\mathrm{i}\boldsymbol{q}\cdot\boldsymbol{r}}\mathrm{d}^3r \\ &= \int_0^\infty\rho_0(\boldsymbol{r}')\mathrm{d}^3r'\int_0^\infty\rho_1(\boldsymbol{u})\mathrm{e}^{\mathrm{i}\boldsymbol{q}\cdot\boldsymbol{r}}\mathrm{d}^3u \\ &= \int_0^\infty\rho_0(\boldsymbol{r}')\mathrm{d}^3r'\int_0^\infty\rho_1(\boldsymbol{u})\mathrm{e}^{\mathrm{i}\boldsymbol{q}\cdot(\boldsymbol{u}+\boldsymbol{r}')}\mathrm{d}^3u \\ &= \int_0^\infty\rho_0(\boldsymbol{r}')\mathrm{e}^{\mathrm{i}\boldsymbol{q}\cdot\boldsymbol{r}'}\mathrm{d}^3r'\int_0^\infty\rho_1(\boldsymbol{u})\mathrm{e}^{\mathrm{i}\boldsymbol{q}\cdot\boldsymbol{u}}\mathrm{d}^3u \\ &= F_0(q)F_1(q), \end{aligned} \tag{15}$$

and

$$F_1(q) = \int\rho_1(r)\mathrm{e}^{\mathrm{i}\boldsymbol{q}\cdot\boldsymbol{r}}\mathrm{d}^3r=\mathrm{e}^{-\boldsymbol{q}^2/2}. \tag{16}$$

We use a trick to make the integration easier, as $\boldsymbol{r}$ is described in the cylindrical coordinate, while $\boldsymbol{q}$ is described in the spherical coordinate as:

$$\left\{\begin{array}{l} x=t\cos\varphi_1 \\ y=t\sin\varphi_1 \\ z=z \end{array}\right\} \quad \left\{\begin{array}{l} q_x=q\sin\theta_2\cos\varphi_2 \\ q_y=q\sin\theta_2\sin\varphi_2 \\ q_z=q\cos\theta_2 \end{array}\right\},$$

then

$$\boldsymbol{qr}=t\cos\phi_1 q\sin\theta_2\cos\phi_2+t\sin\phi_1 q\sin\theta_2\sin\phi_2+zq\cos\theta_2,$$

where $t=\sqrt{x^2+y^2}=\sqrt{r^2-z^2}$.

Thus we obtain

$$\begin{aligned} F_0(q,\theta_2) &= \int\rho_0(r,\theta)\mathrm{e}^{\mathrm{i}\boldsymbol{q}\cdot\boldsymbol{r}}\mathrm{d}^3r=\int\frac{3M}{4\pi a^2b}\mathrm{e}^{\mathrm{i}(xq_x+yq_y+zq_z)}t\mathrm{d}t\mathrm{d}\varphi_1\mathrm{d}z \\ &= \frac{3M}{4\pi a^2b}\int\mathrm{e}^{\mathrm{i}(q\sin\theta_2\cos\varphi_2 t\cos\varphi_1+q\sin\theta_2\sin\varphi_2 t\sin\varphi_1+q\cos\theta_2 z)}t\mathrm{d}t\mathrm{d}\varphi_1\mathrm{d}z \\ &= \frac{3M}{4\pi a^2b}\int_0^a\mathrm{e}^{\mathrm{i}q(t\sin\theta_2\cos(\varphi_2-\varphi_1)+z\cos\theta_2)}t\mathrm{d}t\int_{-\sqrt{\left(1-\frac{t^2}{a^2}\right)b^2}}^{\sqrt{\left(1-\frac{t^2}{a^2}\right)b^2}}\mathrm{d}z\int_0^{2\pi}\mathrm{d}\varphi_1. \end{aligned} \tag{17}$$

The parameters a and b are the semi-axes defined above. Thus the form factor in the EF model can be written as:

$$F(q,\theta_2)=F_0(q,\theta_2)F_1(q). \tag{18}$$

In Fig. 3, the ^{131}Xe density distribution determined by the EF model is shown, while the corresponding form factors are given in Fig. 4. The short dashed-dotted (green) line corresponds to the spherical form of the nucleus. For the spherical nucleus, it has already been known that the form factor obtained with the 2PF model is very close to that determined by the folding model [19]. Thus we will also make a comparison between the E2PF and EF form factors at the end of the paper. Then we will present the third model doing the same job in the following section.

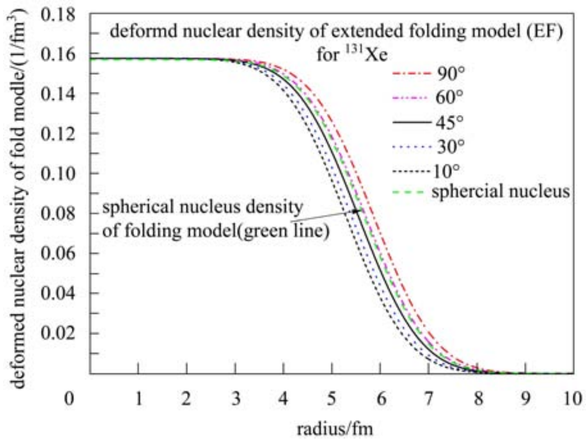

Fig. 3. ^{131}Xe form factors for the deformed nucleus of the extended 2PF(E2PF) model from different directions: 10°, 30°, 45°, 60°, 90°.

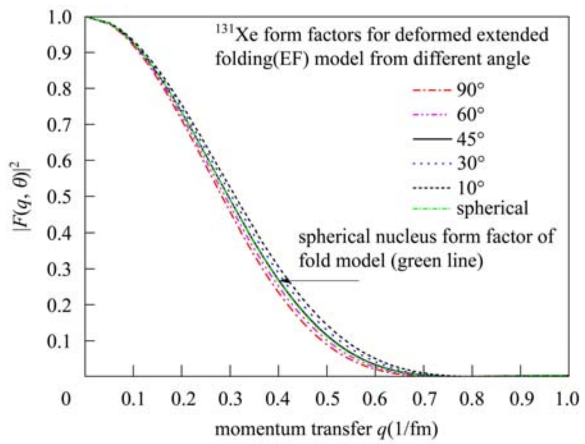

Fig. 4. ^{131}Xe form factors for the deformed nucleus determined in the EF model for different directions: 10°, 30°, 45°, 60°, 90°.

2.3 The Nilsson mean field (NMF)

As mentioned above, we use two simplified models (E2PF and EF) to derive the form factors for the deformed nuclei. The advantage of this is that the models are simple and we can obtain an analytical solution, which is convenient for illustrating the characteristics of the form factors, but might be too simplified. Now we turn to the use a more realistic model.

In this subsection, the form factors for deformed nuclei are obtained in the Nilsson modified oscillator model, and then by using ^{131}Xe as an example, we present the results in some figures.

Below, let us briefly review the model and show how we apply it to study the concerned form factor.

In the Hamiltonian of the Nilsson model, the potential for an axially symmetric harmonic oscillator can be written as [31–33]

$$H=\frac{-\hbar^2}{2M}\nabla^2+\frac{1}{2}M[\omega_x^2(x^2+y^2)+\omega_z^2z^2]-C\boldsymbol{s}\cdot\boldsymbol{l}-D\boldsymbol{l}^2, \quad (19)$$

where $C\boldsymbol{s}\cdot\boldsymbol{l}$ is the spin-orbit coupling, and $D\boldsymbol{l}^2$ flattens the bottom of the potential.

A deformation parameter, δ, is introduced to reflect the axial symmetry for the deformed nuclei as

$$\omega_x^2 = \omega_y^2=\omega_0^2(\delta)\left(1+\frac{2}{3}\delta\right), \quad (20)$$

$$\omega_z^2 = w_0^2(\delta)\left(1-\frac{4}{3}\delta\right). \quad (21)$$

The equipotential surface encloses a constant volume if

$$\omega_x\omega_y\omega_z=\text{const}. \quad (22)$$

Then we have

$$\omega_0\left[1-\frac{4}{3}\epsilon_2^2-\frac{16}{27}\epsilon_2^3\right]^{1/6}=\omega_{00}. \quad (23)$$

The Hamiltonian can be decomposed into three pieces as

$$H = H_{\rm sp}+H_{\epsilon_2}-C\boldsymbol{s}\cdot\boldsymbol{l}-D\boldsymbol{l}^2, \quad (24)$$

$$H_{\rm sp} = \frac{p^2}{2m}+\frac{1}{2}m\omega_0^2r^2, \quad (25)$$

$$H_{\epsilon_2} = -m\omega_0^2r^2\frac{2}{3}\epsilon_2P_2(\cos\theta). \quad (26)$$

It would be convenient to use dimensionless coordinates and parameters that are defined as

$$\rho = \sqrt{\frac{m\omega_0 r}{\hbar}}r, \quad (27)$$

$$C = 2\kappa\hbar\omega_{00}, \quad (28)$$

$$D = \frac{1}{2}C\mu=\kappa\hbar\omega_{00}\mu. \quad (29)$$

Then the Nilsson Hamiltonian can be further written as

$$H = \hbar\omega_0\left(H_0-\frac{2}{3}\epsilon_2P_2\right)$$
$$-\kappa\hbar\omega_{00}\left[2\boldsymbol{s}\cdot\boldsymbol{l}+\mu(\boldsymbol{l}^2-\langle\boldsymbol{l}^2\rangle_N)\right], \quad (30)$$

$$H_0 = \frac{1}{2}(-\nabla_\rho^2+\rho^2), \quad (31)$$

where $\langle\boldsymbol{l}^2\rangle=N(N+3)/2$ is an average over all states within the N-th shell, and $\hbar\omega_{00}\approx 41A^{-1/3}$ MeV.

If the octupole and hexadecupole deformations are considered, the Hamiltonian would become more complicated as

$$H = \hbar\omega_0(H_0+\rho^2(-2/3\epsilon_2P_2+\epsilon_3P_3+\epsilon_4P4))$$
$$-\kappa\hbar\omega_{00}[2\boldsymbol{l}\cdot\boldsymbol{s}+\mu(\boldsymbol{l}^2-\langle\boldsymbol{l}^2\rangle_N)], \quad (32)$$

and it is the Hamiltonian we are going to use in the latter part of this paper.

The Nilsson wavefunction is constructed with the spherical harmonic oscillator basis $|Nlj\Omega\rangle$,

$$\Psi_i = \sum_{\alpha} \omega_\alpha c_\alpha^\dagger |0\rangle, \tag{33}$$

where ω_α is a coefficient, and α refers to a set of quantum numbers, $(njl\Omega)$, of the harmonic-oscillators.

The nuclear density is thus expressed as

$$\rho = \sum_{i=1} (\Psi_i^\dagger(\pi)\Psi_i(\pi) + \Psi_{\bar{i}}^\dagger(\pi)\Psi_{\bar{i}}(\pi)) + \sum_{i=1} (\Psi_i^\dagger(\nu)\Psi_i(\nu) + \Psi_{\bar{i}}^\dagger(\nu)\Psi_{\bar{i}}(\nu)), \tag{34}$$

where $\bar{i}$ represents the time-reversed states.

In this paper, the major shells under consideration are from 0 to 9 for the proton and neutron, respectively. The quadrupole, octupole and hexadecapole deformation parameters are determined by experiments [34], and are -0.108, 0 and 0.027, respectively.

Performing a Fourier transformation on the nuclear density, we obtain the concerned form factor. On the right panel of Fig. 5, the angular dependence of the nuclear density of ^{131}Xe is shown. Fig. 5 plots the NMF form factors $F(q,\ \theta)$ with various angles. The left panel of Fig. 6 compares the form factors at a direction of $\theta = \pi/6$ obtained with the three models: EF, E2PF, and NMF, whereas the right panel shows the corresponding densities. Fig. 7 shows the difference in the form factors $F(q,\ \pi/6)$ for ^{73}Ge and ^{131}Xe, as well as their density distributions.

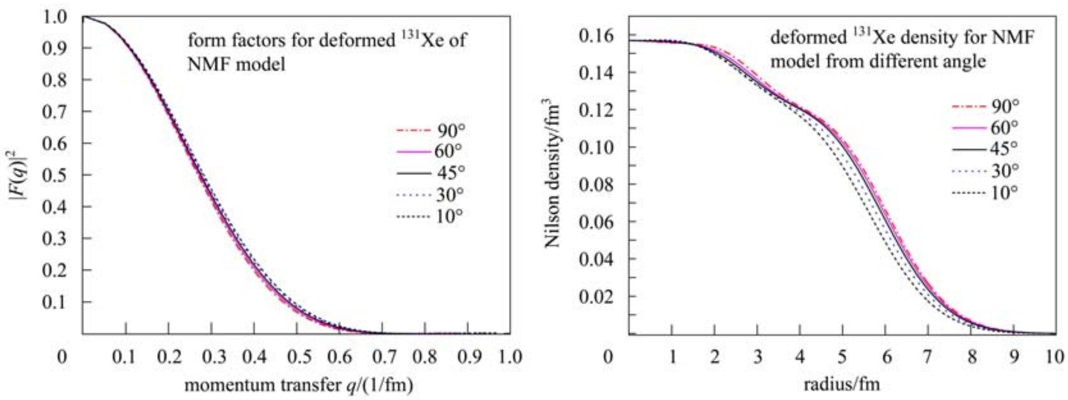

Fig. 5. The right panel shows the dependence of the ^{131}Xe density on the directions from 10° to 90°, obtained in the Nilsson mean field model. The left panel is the form factor.

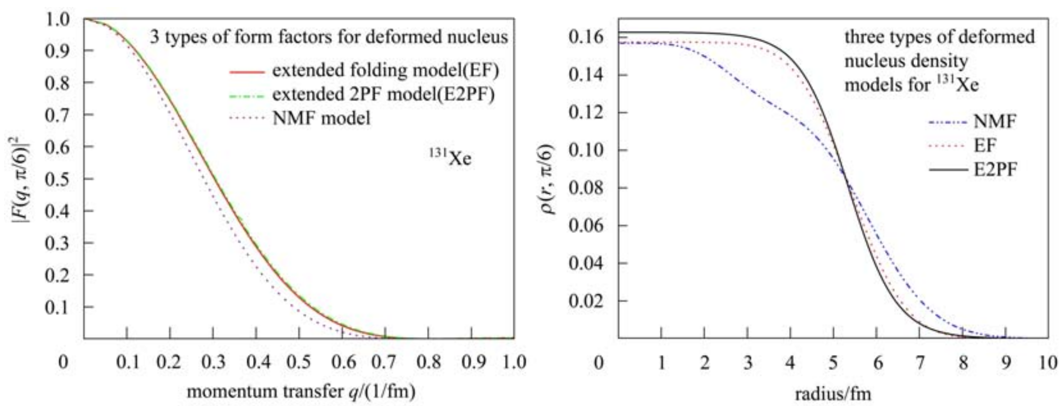

Fig. 6. The form factors $F(q,\ \pi/6)$ and density $\rho(r,\ \pi/6)$ obtained in three different models: E2PF, EF, and NMF for ^{131}Xe.

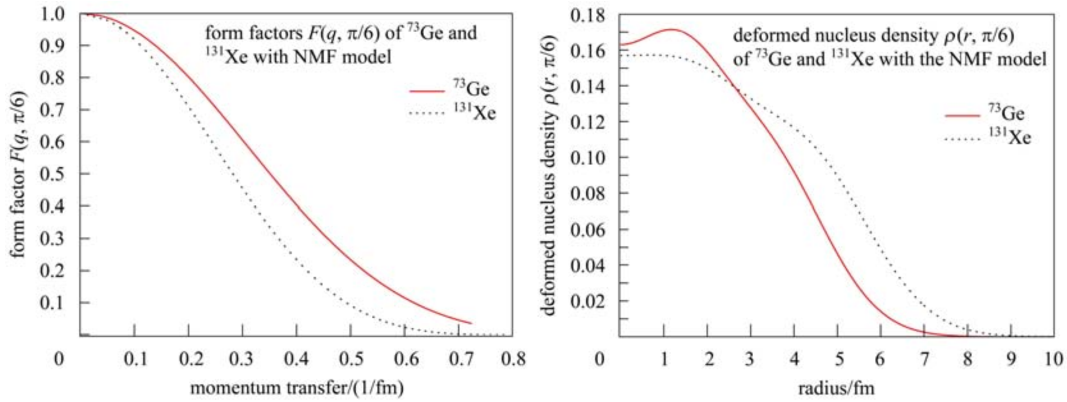

Fig. 7. The left graph shows the form factors $F(q,\ \pi/6)$ for the ^{73}Ge and ^{131}Xe with the NMF model, and the right graph the density distributions $\rho(r,\ \pi/6)$.

3 Summary

The aim of this work was to discover if a small deformation of nuclei can induce observable effects on the form factors for the direct detection of dark matter flux. The form factor, whether the nuclei are of spherical or deformed shape (say ellipsoidal), must satisfy two normalization conditions. First, the nuclear density must be normalized as

$$\int \rho(r,\theta,\phi)\mathrm{d}^3 r = M, \tag{35}$$

where M is the total mass of the nucleus. This is independent of the shape of the nucleus. Second, the form factor must satisfy the condition

$$F(|\boldsymbol{q}|=0)=F(0)=1. \tag{36}$$

This condition does not depend on polar and azimuthal angles. With these two conditions, one can adopt different models for the nuclear density and then carry out a Fourier transformation to convert the nuclear density from the configuration space into the momentum space to gain the form factor which corresponds to non-zero momentum transfer.

In this work, we start with spherical nuclei and adopt three models that are commonly employed to study nuclear effects. Then we extend them to deformed shapes by including polar angle dependence in the density, while an axial symmetry is assumed for simplicity. With the three models, we obtain the form factor for the nuclei whose shape slightly deviates from a spherical form, namely their ellipticity is relatively small.

We notice from the figures shown in the text that the form factors are not far from those for the spherical form, indeed the dependence of the form factor on $|\boldsymbol{q}|$ for $\theta=\pi/4$ is rather close to that for the spherical shape.

In particular, if there is no strong magnetic field to polarize the nuclei at very low temperature, the nuclei in the detection material would be randomly oriented, the polar and azimuthal angles would be averaged and the deformation effects would eventually be smeared out.

Therefore, our conclusion is that unless one can keep the detector at a very low temperature, such as the CDMS detector, and apply a strong magnetic field to it, the effects of the deformation of nuclei can be safely ignored.

References

1 HE X G, Ho S Y, Tandean J, Tsai H C. Int. J. Mod. Phys. D, 2011, **20**: 1423

2 Briscese F. AIP Conf. Proc., 2011, **1396**: 176

3 Briscese F. Phys. Lett. B, 2011, **696**: 315. [arXiv:1101.0028 [astro-ph.CO]]

4 Taoso M, Bertone G, Masiero A. JCAP, 2008, **0803**: 022. [arXiv:0711.4996 [astro-ph]]

5 Cheung K, Mawatari K, Senaha E, Tseng P Y, YUAN T C. Int. J. Mod. Phys. D, 2011, **20**: 1413

6 AN H, CHEN S L, Mohapatra R N, Nussinov S, ZHANG Y. Phys. Rev. D, 2010, **82**: 023533. [arXiv:1004.3296 [hep-ph]]

7 Fornengo N, Scopel S, Bottino A. Phys. Rev. D, 2011, **83**: 015001

8 Morselli A. Prog. Part. Nucl. Phys., 2011, **66**: 208–215

9 Profumo S. AIP Conf. Proc., 2009, **1182**: 256–258

10 Sonnenschein L. [arXiv:1106.4901 [hep-ex]]

11 Jungman G, Kamionkowski M, Griest K. Phys. Rept., 1996, **267**: 195. [arXiv:hep-ph/9506380]

12 Goodmand M W, Witten E. Phys. Rew. D, 1986, **31**: 3059

13 Ressell M T, Aufderheide M B, Bloom S D, Griest K, Mathews G J, Resler D A. Phys. Rev. D, 1993, **48**: 5519

14 Ressell M T, Dean D J. Phys. Rev. C, 1997, **56**: 535–546. [hep-ph/9702290]

15 Engel J, Vogel P. Phys. Rev. D, 1989, **40**: 3132–3135

16 Engel J. Phys. Lett. B, 1991, **264**: 114–119

17 Drees M, SHAN C L. PoS, 2008, **IDM2008**: 110. [arXiv:0809.2441 [hep-ph]]

18 Duda G, Kemper A, Gondolo P. JCAP, 2007, **0704**: 012

19 CHEN Y Z, LUO Y A, LI L, SHEN H, LI X Q. Commun. Theor. Phys., 2011, **55**: 1059–1064. [arXiv:1101.3049 [hep-ph]

20 Brown M J, Greiner W. Z. Phys. A, 1983, **310**: 287

21 Ismail M, Gealy E L. Phys. Lett. B, 2003, **563**: 53

22 Cooper T, Bertozzi W et al. Phys. Rev. C, 1976, **13**: 1083

23 XU C, REN Z Z. Phys. Rev. C, 2006, **73**: 041301

24 Walecka J D. Theoretical Nuclear Physics and Subnuclear Physics. Oxford: Oxford University Press, 1995. 11–13

25 Hahn B, Ravenhall D G, Hofstadter R. Phys. Rev., 1956, **101**: 1131

26 Bohr A, Mottelson B R. Nuclear Structure. Singapore: World Scientific, 1998. 1

27 Ismail M, Seif W M, Ellithi A Y, Salah F. J. Phys. G, 2008, **35**: 075101

28 Moller P et al. Atom Data and Nuclear Data, 1995, **59**: 185–381

29 Helm R. Phys. Rev., 1956, **104**: 1466

30 Lewin J D, Smith P F. Astropart. Phys., 1996, **6**: 87

31 Nilsson S G et at. Nucl. Phys. A, 1969, **131**: 1

32 Mottelson B R, Nilsson S G. Phys. Rev., 1958, **99**: 1615

33 Nilsson S G. Mat. Fys. Medd. Dad. Vid. Selsk., 1955, **59**: 185–381

34 http://t2.lanl.gov/data/astro/molnix96/massd.html